ROTATIONAL RELAXATION OF NITROGEN IN A FREE JET OF ARGON

A. E. Belikov, G. V. Dubrovskii, A. E. Zarvin,
N. V. Karelov, V. A. Pavlov, P. A. Skovorodko,
and R. G. Sharafutdinov

UDC 533.6.011.8

The collisional exchange of energy for rotational movement of molecules is studied a great deal both theoretically and experimentally. This is connected both with traditional problems about dispersion and absorption of ultrasound, thermal transpiration, and determination of transfer coefficients, and with comparatively new problems of calculating population kinetics for rotational levels in molecular gas masers, determination of mechanisms of cosmic laser emission, and also with other problems, where information is important not just about the rates of rotational energy transfer for the system as a whole, but about populations of individual quantum states.

Currently, in order to describe population kinetics for rotational levels in expanding streams use is made only of the hydrodynamic method of description [1-4], although it is well known that the typical times for establishing equilibrium for translational and rotational degrees of freedom for the majority of gases are comparable, which places doubt on the applicability of this method. In addition, in these works use was made of a parametric form for dependences of microscopic rate constants on temperature and quantum numbers with parameters selected from experiments. Therefore, this comparison of experiments and calculations does not make it possible to develop the possibility of using the hydrodynamic description method and to make a selection of rate constants. The difficulty of selecting one or another type of constant is clearly demonstrated in [4]. Description of experimental data obtained in these works may be preferably considered as a compact representation of them, but not as a theoretical description.

More consistent comparison of theory with experiment may be carried out with independent calculation of rate constants by the method of dispersion theory. In this work, an attempt is made to carry out this approach on the example of a collision pair of nitrogen–argon, whose selection is connected with the possibility of excluding from consideration translational–rotational transitions and using the method of electron-beam diagnostics, making it possible to obtain detailed information about populations of rotational levels for nitrogen. In addition, for a nitrogen–argon pair, recently quite a large number of calculations have been carried out for cross sections of relatively inelastic collisions, which makes it possible to estimate the reliability of the rate constants used. As a gasdynamic object, in which nonequilibrium of the process is observed, the core of a free argon jet with a small nitrogen impurity was selected. In the core of the jet, flow, which in [5] corresponds to outflow of gas into a vacuum, gas density and collision frequency fall very rapidly and, therefore, a change in internal energy does not manage to follow a reduction in the translational temperature; i.e., there is a delay in the relaxation process until it is frozen at some distance from the nozzle edge. The aim of this work is comparison of experimental data for population kinetics for rotational levels in the axis of the jet with values calculated from a rotational relaxation model, which makes it possible to estimate the validity both of the relaxation process model selected and use of rate constants.

1. Kinetic Equations. In a hydrodynamic approximation [6] for unidimensional steady flow of a stream in a tube taking account only of rotational–translational energy exchange for a small admixture of nitrogen in argon, the set of kinetic equations has the form

$$u\frac{dN_k}{dx} = n_{\mathrm{Ar}}\sum_{\Delta k}\{[K_{k+\Delta k,k}N_{k+\Delta k} - K_{k,k+\Delta k}N_k] - [K_{k,k-\Delta k}N_k - K_{k-\Delta k,k}N_{k-\Delta k}]\}, \quad (1.1)$$

Novosibirsk. Translated from Zhurnal Prikladnoi Mekhaniki i Tekhnicheskoi Fiziki, No. 5, pp. 19-29, September-October, 1986. Original article submitted July 9, 1985.

0021-8944/86/2705-0643$12.50

where x is distance of the stream along the tube; u is gas velocity; n_{Ar} is numerical density for argon; $N_k = n_k/\Sigma n_k$ is relative population of the k-th rotational level; K_{ij} are microscopic equilibrium rate constants. Due to the strict prohibition of collision transitions between ortho and para modification of nitrogen only transitions with even values of Δk are resolved. Therefore, the set of equations (1.1) breaks down into two unconnected sets for even and uneven levels.

In accordance with the principle of detailed equilibrium, the set of Eqs. (1.1) is transformed

$$u\frac{dN_k}{dx} = n_{Ar}\sum_{\Delta k}\left\{K_{k+\Delta k,k}\left[N_{k+\Delta k} - N_k\left(\frac{N_{k+\Delta k}}{N_k}\right)_t\right] - K_{k,k-\Delta k}\left[N_k - N_{k-\Delta k}\left(\frac{N_k}{N_{k-\Delta k}}\right)_t\right]\right\}.$$

The value

$$\left(\frac{N_{k+\Delta k}}{N_k}\right)_t = \frac{2(k+\Delta k)+1}{2k+1}\exp\left[-\Delta k(2k+\Delta k+1)\frac{\Theta}{T_t}\right]$$

represents the ratio of populations for rotational levels of molecules with their equilibrium distribution with temperature equal to the translational temperature of the gas T_t. Here $\theta = 2.878$ K is the rotational constant for the zero vibration level of nitrogen. It was assumed that the distribution of density, velocity, and translational temperature along the axis of the jet for an axisymmetric sonic nozzle is the same as with expansion of an ideal gas with ratio of heat capacities $\gamma = C_p/C_V = 5/3$. Relationships u(x), n(x), $T_t(x)$ were found by numerical solution of a set of gasdynamic equations similar to that in [7]. Furthermore, it was assumed that in the subsonic part of the nozzle equilibrium occurs between the translational and rotational degrees of freedom, and in the geometric section of the nozzle the Mach number calculated from the equilibrium sound velocity equals unity. Calculation was started from the edge of the nozzle where an equilibrium distribution of molecules for the rotational level was prescribed. In the calculation 56 rotational levels were considered. The rest of the details of the calculation are given in [4].

2. Cross Sections and Rate Constants. In a theoretical analysis of the effectiveness of rotational transitions in molecules one comes up against the following problems: approximation of the reaction potential, selection of a method for working out cross sections and building up analytical approximations for rate constants over a sufficiently wide range of change in quantum numbers and gas temperature, embracing the range of change of these values for the experiment. All of this makes a very difficult task of obtaining final (working) equations for rate constants and explains the fact that, first, the number of practically realized equations is very small and, second, they require careful comparison with each other and checking, even if the original theoretical method of working out cross sections permits a strict evaluation of its accuracy.

The reaction potential in the system N_2 + Ar is presented in the form

$$W(R, \gamma) = W_0(R) + W_2(R)\cos^2\gamma, \tag{2.1}$$

where R is distance between Ar atoms and the center of mass for an N_2 molecules; γ is angle between the rotator axis and lines joining the atom with the center of mass of the molecule. Function $W_{0,2}(R)$ was determined in one case by the method suggested in [8], and in another by comparing (2.1) with numerical calculations for potential surfaces [9]. As a result of this, approximations (in an atomic system of units) are obtained:

$$W_0(R) = W_2(R) = Ce^{-\alpha R},\ C = 1{,}8\cdot 10^5\ \alpha = 2{,}9; \tag{2.2}$$

$$W_k(R) = \varepsilon_k\left[\left(\frac{\sigma_k}{R}\right)^{12} - \left(\frac{\sigma_k}{R}\right)^{6}\right],\ \varepsilon_0 = 2\cdot 10^{-3},\ \sigma_0 = 5{,}8,\ \varepsilon_2 = 6\cdot 10^{-4},\ \sigma_2 = 7{,}2,\ k = 0{,}2. \tag{2.3}$$

In order to work out the effectiveness of rotational reaction, use was made of an expression for the complete cross section in the form of an integral for impact parameter b from the "profile of inelastic scattering" (Bessel approximation) [10]:

$$\sigma_{jj'}(E) = 2\pi\left(\frac{2j+1}{2j'+1}\right)^{1/2}\left(\frac{E-E_*}{E}\right)^{1/2}\int_0^\infty dbbI^2_{\frac{\Delta j}{2}}\left[\frac{F(R_0(b))}{\hbar}\right]. \tag{2.4}$$

Here j and j' are initial and final rotational quantum numbers; $\Delta j = |j - j'|$; E_* is relative efficiency; R_0 is radius-vector modulus for the point of greatest approximation of particles. Expression (2.4) is derived from a strictly quasiclassical representation of the T-operator in angle–effect variables in a first-order perturbation theory for a classical increase in effect [11]. In obtaining it and subsequent expressions for F, use was made of simplifying assumptions; no consideration was given to the effect of the rotator on relative movement (approach of an external force); consideration was only given to plane rotator configurations; in calculating $W_2[R(t)]$ close to the point of greatest approach, use was made of a rectilinear movement trajectory R(t) [12]. On these assumptions the argument of the Bessel function in (2.4) is written as

$$F = -\int_{-\infty}^{+\infty} dt\frac{W_2[R(t)]}{2}\cos 2\hat{\nu}t,$$

where $\hat{\nu} = (\nu + \nu')/2 = B_e(j + j' + 1)$ is average unperturbed frequency for rotator rotation (B_e is rotational constant for the molecule); $R^2(t) = X^2(t) + Y^2(t)$; $X(t) = R_0$; $Y(t) = \hat{\nu}t$.

Within the framework of the assumptions indicated above, function F for the Lennard–Jones W_2 potential (2.3) was calculated in explicit form:

$$F = F^> - F^<, \quad F^{\gtrless} = \frac{\sqrt{\pi}\,W_2^{\gtrless}(b)\,\eta^{S^{\gtrless}+1}}{\Gamma\left(S^{\gtrless}+\frac{1}{2}\right)\hat{\nu}2^{S^{\gtrless}+1}}K_S^{\gtrless}(\eta),$$

$$W_2^{\gtrless}(R) = \varepsilon_2\left(\frac{\sigma_2}{R}\right)^{2S^{\gtrless}+1}, \quad \eta = \frac{2\hat{\nu}b}{\hat{v}}, \quad S^< = \frac{5}{2}, \quad S^> = \frac{11}{2}.$$

Here Kq(x) is the MacDonald function; Γ(x) is the gamma function. Furthermore, in the calculation consideration was only given to the attracting part of the potential and, in the vicinity of point b_0, where the Bessel function has the principal maximum, use was made of a stepped approximation for $F(\eta)$. Calculations were carried out in explicit form and they gave simple analytical equations

$$F = C_1\frac{\sqrt{\pi}}{2^{15/4}}\mu^{3/4}\hat{\nu}^{1/2}\hat{E}^{-3/4}b^{-9/2}, \quad C_1 = \frac{\varepsilon_2}{4}\sigma_2^{2S^<+1}, \tag{2.5}$$

$$\sigma_{jj'}(E) = 2\pi\sigma_*\left[\frac{E-E_*}{E}\frac{2j'+1}{2j+1}\right]^{1/2}\frac{(j+j'+1)^{2/9}}{\hat{E}^{1/3}}\frac{\Gamma\left(\frac{\Delta j}{2}-0{,}2\right)}{\Gamma\left(\frac{\Delta j}{2}-1{,}4\right)}$$

[$\hat{E} = (E + E')/2$ is average energy, μ is proposed mass).

After averaging for Maxwellian distribution of cross sections (2.5), an equation is obtained for equilibrium rate constants:

$$K(j \to j', T) = \left(\frac{8}{\pi\mu}\right)^{1/2}(kT)^{0{,}2}\sigma_* e^{-\Theta_*}I(\Theta_*), \tag{2.6}$$

where

$$\Theta_* = \frac{B_e[(j'+1)j' - (j+1)]}{kT}; \quad I_*(\Theta_*) = 0{,}9314(1 + 1{,}24\Theta_*)^{0{,}3}.$$

The value of constant σ_* is given below. In the range of parameters for the experiment

$$I(\Theta_*) = 0{,}9314(1 + 1{,}24\Theta_*)^{0{,}3}.$$

The working equation in the SI system is

$$K_{\cdot}(j \to j', T) = 1{,}224 \cdot 10^{17} T^{0,3} \left(\frac{2j'+1}{2j+1}\right) \frac{\Gamma\left(\frac{\Delta j}{2} - 0{,}2\right)}{\Gamma\left(\frac{\Delta j}{2} + 1{,}4\right)} e^{-\Theta_* I}(\Theta_*).$$

3. Comparison of Calculations for Flow and Constants with Other Data. In comparing cross sections obtained by different methods, attention should be drawn to the marked role of potential surface on these values. In works with which the comparison was carried out use was made of two models for potential surface, i.e., short reaction (SR-model) [13] and long reaction (LR model) [14].

A comparison is given in Table 1 for cross sections of transitions from j = 0 into j' in units of 10^{-16} cm^2 with four values of energy of translational movement. In calculating cross sections by simplified Eq. (2.5) the value of σ_* was selected from conditions for conformity with calculations [16] with T = 300 K for the transition 0 → 2 (σ_* = 1.9). Here, in lines 8 and 9, a comparison is given for rate constants with a translational temperature of 300 K. Constants are given in units of 10^{-10} cm^3/sec. It can be seen that the selection of potential surface with the same calculation method determines both the values of the overall cross section and its dependence on Δj (lines 4-7).

Simplified Eq. (2.5) gives a sharper reduction in cross section with an increase in Δj at 300 K than Eq. (2.4) and the strong bond (SB) method. Rate constants, according to Eq. (2.6) with T_t = 300 K for the transition 0 → 2, are close in value to data in [18], although the drop for Δj in [18] is steeper than for (2.6). On the whole, the order of rate constants and cross sections used in the present work conforms with data in the literature.

4. Experimental Procedure. Experiments were carried out in a low-density gasdynamic unit at the Thermal Physics Institute, Siberian Section, Academy of Sciences of the USSR fitted with electron beam diagnostics for measuring gas density and the populations of rotational levels for nitrogen molecules. Detailed description of the equipment is given in [19], and the electron-beam measurement procedure is given in [20].

Evacuation of the gasdynamic unit was accomplished by oil–vapor and cryogenic pumps. The pressure level of the background gas in all of the measurements did not exceed 0.4 Pa, which makes it possible to ignore penetration of it into the jet axis.

Axisymmetric sonic nozzles with a diameter at the edge d_* = 5.11 and 15.0 mm served as gas sources. The mixing chamber of the nozzle was placed in a resistance heater in the form of two coaxial silica tubes with a small gap containing a Nichrome spiral winding heated

TABLE 1

Test No.	E, K	σ, h: 2	4	6	8	10	Potential model	Method	Equation	Source
1	300	22,3	19,1	12,7	4,9			SB		[15]
2		26,8	9,7	1,3	0,06		(2.2)		(2.4)	[16]
3		26,8	10,7	6,6	2,4				(2.5)	
4		26,7	22,8	10,1	1,16			SB		[17]
5		22,6	23,5	10,4	1,25					[17]
6		59,1	15,2	0,32				SB		[17]
7		58,2	2,07	0,03						[17]
8	300	1,27	0,52	0,28	0,16	0,31			(2.6)	
9		1,6	0,21	0,014						[18]
1	450	17,5	14,0	12,4	6,1	1,96		SB		[15]
2		24,2	15,1	3,7	0,4	0,02	(2.2)		(2.4)	[16]
3		19,4	9,7	6,3	2,8	1,75			(2.5)	
1	618	16,0	13,4	11,8	4,5	0,58		SB		[15]
2		20,5	18,1	7,1	1,3		(2.2)		(2.4)	[16]
3		17,8	9,0	6,1	3,0	2,02			(2.5)	
1	768	15,7	11,4	10,8	5,7	1,15		SB		[15]
2		17,9	18,3	9,96	2,57	0,35	(2.2)		(2.4)	[16]
3		16,66	8,49	5,79	2,85	2,06			(2.5)	

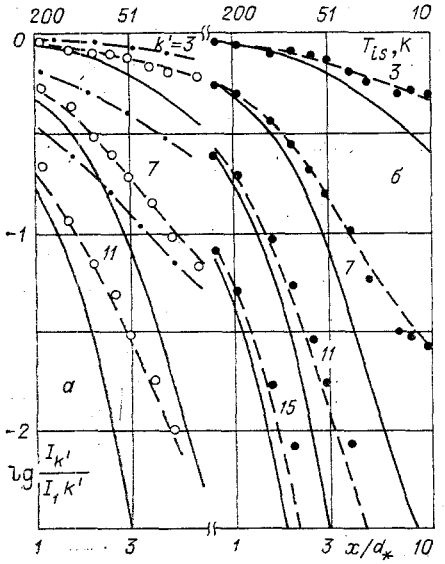

Fig. 1

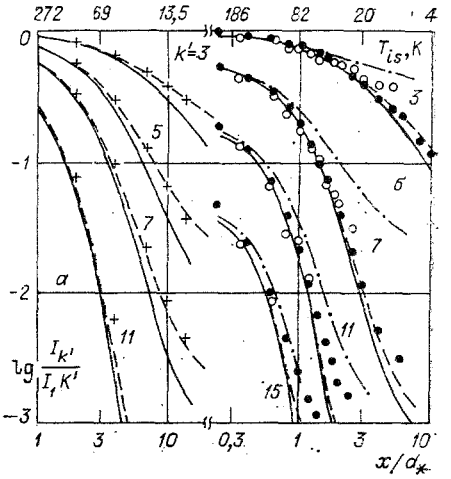

Fig. 2

TABLE 2

Schedule	T_0, K: Delivery method	T_0, K: By measuring density with an optical method	T_0, K: By measuring density by an X-ray method	T_0, K: Thermocouple	T_0, K: Value adopted in the calculation	$p_0 d_*$, N/m	Re_0	M_t	$(x/d_*)_t$: By an equation from [21]	$(x/d_*)_t$: $P_B>0,3$ (by Eq. (7.1))	$(x/d_*)_t$: $P_B>0,3$ ($\sigma=40\cdot10^{-16}$ cm)	d_*, mm	n_{N_2}: $n_{N_2}+n_{Ar}$	Figure
1	730	958	—	890	730	6.65	378	10.5	6.2	2	3.5	5.11	0.06	1,a
2	730	879	931	835	730	12.24	700	13.5	8.85	3	9	5.11	0.05	1,b
3	990	1140	1160	1040	990	96.7	3500	25.8	24.2	7	10	5.11	0.05	2,a
4				293	293	1.22	274	8.4	4.5	1,2	3	15	0.04	2,b
5				293	293	18.6	4190	25	21.8	5,5	10	15	0.06	2,b

by a current. The test gas entered the mixing chamber through this region, thus heating it during its passage. Gas temperature in the mixing chamber was measured by a platinum–platinum–rhodium thermocouple located close to the nozzle. Measurement of stagnation pressure was accomplished by U-shaped manometers filled with organosilicon liquid, and also by vacuum gauges VO-1277 with a 0.25 accuracy class. Apart from thermocouple measurements, the stagnation temperature was determined by the delivery method, and by measuring the density by optical and x-ray electron-beam methods.

With a constant delivery through the nozzle, the stagnation temperature of the heated gas may be calculated from the relationship

$$T_{02} = \left(\frac{p_{02}}{p_{01}}\right)^2 T_{01},$$

where p_0 and T_0 are stagnation pressure and temperature; an index 1 indicates a gas parameter at room stagnation temperature, and 2 indicates heated gas. This relationship was obtained assuming absence of an effect of viscosity and heat exchange in the precritical part of the nozzle.

By assuming that the ratio of densities at the x axis of a free jet n/n_0 does not depend on the value of the stagnation temperature, we obtain

$$T_{02} = \left(\frac{n_1}{n_2}\right)\left(\frac{p_{02}}{p_{01}}\right) T_{01}.$$

The ratio of densities for cold and hot gas n_1/n_2 at a constant distance from the nozzle edge was measured by optical and x-ray emission excited by a mean of electrons.

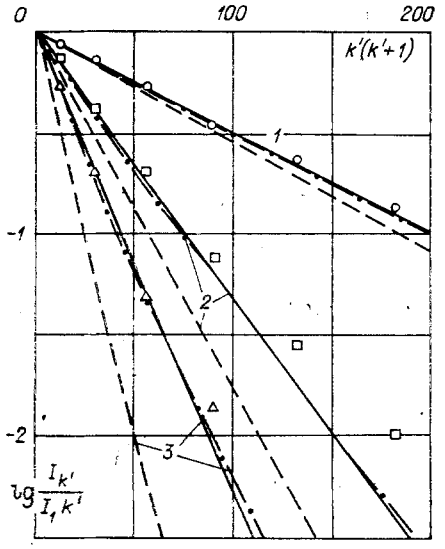

Fig. 3

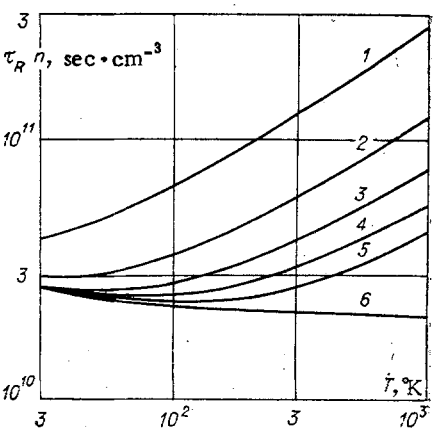

Fig. 4

5. Experimental Results and Comparison with Calculations. The experimental conditions are given in Table 2. In order to estimate the effect of a boundary layer in the nozzle, from data in [21] values of the number $Re_0 = \rho_0 a_0 d_* / \mu_0$ are given calculated from stagnation parameters. Examples of measured results and calculations are given in Figs. 1 and 2 in the form of intensities for rotational lines of the first negative system of lines $I_{k'}$, normalized into a derivative for intensity of the first line by number k' (k' is rotational quantum number in the $N_2^+ B^2\Sigma_u^+$, v' = 0 state), in relation to prescribed distance x/d_*. Calculated values for line intensities were obtained by the equation

$$I_{k'} = P_{k'k''} \sum P_{kk'} N_{kv}$$

where $P_{k'k''}$ is the Henley–London emission factor ($B^2\Sigma \to x^2\Sigma$); $P_{kk'}$ is the probability of rotational transitions from k to k' with $x'\Sigma$, v = 0 → $B^2\Sigma$, v' = 0 by electron transition initiated by an electron beam. Values of $P_{kk'}$ were taken from [20]. Populations of levels in the $x^1\Sigma$, v = 0 state were found by solving the set of kinetic equations (1.2) for rate constants in the form (2.6). Solid lines in Figs. 1 and 2 give calculations for equilibrium isoentropic flow with $\gamma = 5/3$, and broken lines give this solution of the set of kinetic equations (a broken-dotted line in Fig. 1a is the calculation ignoring all of the transitions with N_2 + Ar collisions, apart from $\Delta k = \pm 2$), and points are experimental data. Open points in Fig. 2b are schedule 4, and shaded parts are schedule 5. Calculated values of the translational temperature are applied at the top of Figs. 1 and 2.

On the whole, both calculated and experimental results correspond with contemporary ideas about the kinetics of rotational relaxation in an expanding gas: in the initial stage of expansion, the intensity of lines (consequently, the populations of levels in the $x^1\Sigma$ state) is close to the equilibrium value. Deviation from equilibrium, caused by rapid cooling of the gas and a reduction in collision frequency at reduced density, increases gradually as the distance from the nozzle edge increases. With a high stagnation temperature closest of all to equilibrium flow, data are found with maximum $p_0 d_*$ (schedule 3, Fig. 2a), and the most nonequilibrium distributions occur with the minimum $p_0 d_*$ (schedule 1, Fig. 1a). Satisfactory conformity is observed between calculation and experiment at the lower levels, although it should be noted that the higher the rotational level, the greater the difference between calculation and experiment.

There is no agreement between theory and experiment with room-temperature stagnation. Theory predicts more nonequilibrium distributions of populations than there are in the experiment. According to estimates based on calculations with different $n_0 d_*$, the rate of the relaxation process for the lower levels (k < 7) predicted by theory is three to four times lower than that in the experiment. Comparison of theory and experiment with room-temperature stagnation is carried out in the same range of translational temperature in the stream as with elevated stagnation temperatures and, therefore, these differences are not connected with values of rate constants and with different expansion prehistory on reaching the same

values of translational temperature for the gas in the heated form and with room-temperature stagnation, which is confirmed by calculations with different $p_0 d_*$ (see Figs. 1 and 2). The reason for such a marked difference between theory and experiment with room-temperature stagnation is not clear, and it is only possible to suggest the role of van der Waals molecules not considered in the rotational relaxation model.

The contribution of multiquantum transitions ($\Delta k > 2$) in describing the kinetics of populations is shown in Fig. 1a, where a comparison is made of calculations taking account of transitions only for $\Delta k = \pm 2$ (dotted-broken curves) and taking account of all of the transitions (broken curves).

The role of transitions with $\Delta k > 2$ is significant and more marked for flow far from equilibrium. For flow close to equilibrium, differences in calculations with $\Delta k = \pm 2$ from those calculated taking account of all transitions are insignificant.

6. Time of Rotational Relaxation. Analysis of calculated distributions for populations of levels indicates that they are close in form to Boltzmann distributions, which implies the possibility of their approximate description by a single rotational temperature. An example of these distributions is given in Fig. 3 for three distances from the nozzle edge with $T_0 = 800°K$ and $p_0 d_* = 13.6$ Nm^{-1}, line 1 ($x/d_* = 1.01$, $T_t = 217°K$, $T_R = 239°K$), 2 ($x/d_* = 2.95$, $T_t = 57°K$, $T_R = 81°K$), 3 ($x/d_* = 6.8$, $T_t = 18°K$, $T_R = 41.5°K$).

Broken lines are the distribution of line intensities with a Boltzmann distribution in the $X^1\Sigma$, $v = 0$ state, broken-dotted lines are the results of calculation for a set of kinetic equations, points are for the experiment, and solid lines are for calculations of rotational temperature from the relaxation equation

$$u\frac{dT_R}{dx} = \frac{T_{is} - T_R}{\tau_R}. \tag{6.1}$$

The time for rotational relaxation was calculated for the case of small deviations from equilibrium in rate constant (2.6) similar to [4]. It can be seen from Fig. 3 that for calculating the kinetics of populations it is possible to use a single rotational temperature not only for small deviations from equilibrium, but for significant ones.

The contribution of individual channels to the value of rotational relaxation time is shown in Fig. 4, where calculations of $n\tau_R$ are given, taking account only of two quantum transitions ($\Delta k = \pm 2$), two and four quantum transitions, etc. (curves 1-6, respectively). It can be seen that the role of multiquantum transitions is most marked at high temperatures and it gradually decreases as temperature decreases. Similarly for the effect of multiquantum transitions on population kinetics, the lower the temperature in the stream, the less marked is the effect of multiquantum transitions.

It should be noted that the approximate description of population kinetics for levels by means of rotational temperature is a consequence of the type of constant. For another selection of rate constants there may be no similar description [4].

7. Analysis. In comparing theory with experiment, the following assumptions were made: no importance for the effect of impurities both on gasdynamic parameters and on the population kinetics for levels; no importance for excitation of vibratory degrees of freedom; validity of hydrodynamic approximation in describing nonequilibrium gasdynamics; validity of isoentropic relationships for flow of a monatomic gas for an axial tube of flow; validity of the selection of the delivery method in order to determine the stagnation temperature. Briefly we analyze each of the assumptions made.

Experiments carried out with room-temperature stagnation, with constant $p_0 d_* = 65$ Nm^{-1}, and different molar fractions of nitrogen, showed that with a nitrogen fraction less than 0.07 the population kinetics in the range of measurement error do not depend on the amount of nitrogen in the mixture. The molar fraction of nitrogen in the mixture in all of the experiments carried out did not exceed 0.06. Calculations taking account of this amount of impurity with a ratio of heat capacities for the mixture

$$\frac{\gamma}{\gamma - 1} = C_1 \frac{\gamma_1}{\gamma_1 - 1} + C_2 \frac{\gamma_2}{\gamma_2 - 1}$$

(C_i and j_i are molar fraction and ratio of component heat capacities) also confirmed the unimportance of its effect on gasdynamic parameters and the distribution of population levels. With the maximum stagnation temperature in this work (1000 K) the ratio of populations for

the first vibratory level in the $X^1\Sigma$ state to population of the zero level equals 0.04. In theoretical calculation of line intensities this contribution was ignored. We estimate how much this is valid for the maximum. Emission intensities for rotational lines of the band 00 (v' = 0, v" = 0) are connected with population levels in the $X^1\Sigma$ state by the relationship

$$I_{k'k''} = C\left(q_{00}\sum_k P_{kk'}^{v=0}N_k^{v=0} + q_{10}\sum_k P_{kk'}^{v=1}N_k^{v=1}\right),$$

where the first term takes account of excitation by electron shock of the zero level, and the second term takes account of the first vibratory level in the $X^1\Sigma$ state; q_{00} and q_{10} are the probabilities of electron vibratory transitions from $X^1\Sigma$, v into $B^2\Sigma$, v', and $P_{kk'}{}^{v}$ is the probability of electron-vibratory rotational transitions in the same electron transition. Constant C contains all of the values not depending on k, k', and v. We assume that the vibratory relaxation of nitrogen is frozen at the stagnation temperature, q_{00} and q_{10} equal the Franck–Condon factor [22], and $P_{kk'}{}^{v=1} = P_{kk'}{}^{v=0}$. By taking the value of $P_{kk'}{}^{v=1}$ the same as in [20], we find that the contribution of excitation in the first vibratory level to the intensities of individual rotational lines is less than 0.4%, and they may be ignored in the whole of the test temperature range.

In the theoretical description it was assumed that disruption of a Maxwellian distribution for rates of translational movement of molecules is insignificant, and in order to describe the dynamics of a nonequilibrium gas a hydrodynamic approximation with retarded relaxation is valid [6], using microscopic equilibrium rate constants. However, it is well known that the typical times for establishing translational and rotational relaxation are comparable. We estimate for each of the experiments the distance from the nozzle edge at which disruption is possible for translational equilibrium. First this is done on the basis of an empirical equation from [21] for the value of local Knudsen number [23]. For the start of translational equilibrium disruption we take a point where with equilibrium isentropic expansion a limiting Mach number is reached [21]

$$M_t = 1{,}17\mathrm{Kn}_*^{-(\gamma-1)/\gamma}.$$

Here Kn_* is the Knudsen number determined from the line for free travel in the critical cross-section of the nozzle. The gas-kinetic cross section for argon was calculated by the equation

$$\sigma = \pi(2{,}99)^2(1 + 142/T)10^{-20}\ [\mathrm{m}^2]. \qquad (7.1)$$

The value of M_t and the distances where it is achieved with equilibrium expansion are given in Table 2. In obtaining the second estimate we shall assume the following from [23]: that disruption of translational equilibrium commences with a local Knudsen number $P_B \gtrsim 0.3$. In calculating P_B the gas-kinetic cross section was taken either from Eq. (7.1), or with a constant value ($\sigma = 40\cdot10^{-10}$ m^2). Although the estimate gives quite considerable scatter, in all of the experiments at elevated stagnation temperature the start of translational equilibrium disruption sets in much lower along the stream than the start of disruption for the Boltzmann distribution in that range of distances from the nozzle where comparison of theory and experiment was carried out. Consequently, the assumption about the applicability of hydrodynamic approximation for these conditions may be assumed to be valid. For experiments with room-temperature stagnation, according to estimates the start of translational equilibrium disruption is observed where deviation starts from rotational–translational equilibrium.

In the theoretical description of population kinetics for levels it was assumed that the dependences for density, rate, and translational temperature on coordinates along the

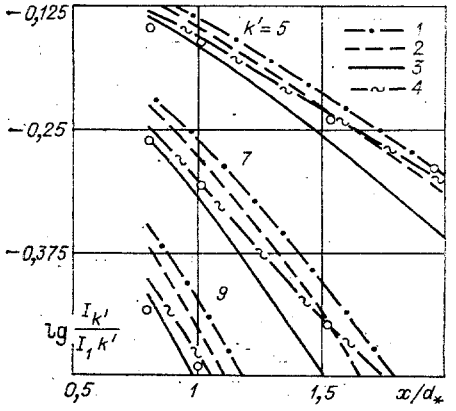

Fig. 5

jet axis are governed by a set of isentropic expansion equations for monatomic gas. In the calculation as initial conditions it was assumed that the planar surface with M = 1 is in a geometrically critical cross section of the nozzle. This assumption is not valid for the whole of the stream in the core of the jet. Theoretically [24] and experimentally [21, 24] it has been demonstrated that a surface with M = 1 is not planar and delivery coefficient depends strongly on the shape of the subsonic part of the nozzle. In particular, for an opening in a thin wall (our case is close to this) it approximates to 0.856 [24]. In these works it was noted that the shape of the subsonic part of the nozzle does not markedly alter the flow in the jet axis. Measurement of population levels carried out with a room temperature for stagnation by the combined scattering method [25] and by an electron beam [26] confirm satisfactorily the isentropic calculations for the jet axis, at least with distances $x/d_* > 0.8$. Data in Fig. 2a, where calculations and experiments conform in the equilibrium part of flow, may serve as confirmation of the applicability of the isentropic calculation for the axis. Populations of the upper levels (and, consequently, line intensities) are very sensitive to the amount of temperature deviation from the calculated value.

The effect of friction and heat exchange in the subsonic part of the nozzle may also lead to a difference in actual flow from the calculated value. For nozzles made in the form of a hole in a thin wall, with a wall temperature equal to the stagnation temperature, the effect of flow is not marked with $Re_0 > 100$ [21] (all of the Re_0 values in this work are above this).

As can be seen from Table 2, different values of stagnation temperatures determined by the difference method do not coincide; the highest T_0 were calculated from the measured densities from optical and x-ray studies, and the minimum values were calculated by the delivery method. This difference in T_0 values decreases with an increase in Re_0. In comparing theory with experiment, values of the delivery method were taken as calculated values of T_0. We substantiate this choice. Plotted in Fig. 5 for schedule 2 are the intensities of lines with $k' = 5, 7, 9$ for distances close to the nozzle edge (points). The selection of these lines was made for the reason that, in distances close to the edge, populations of the corresponding levels differ little from the equilibrium values, but they are quite sensitive to T_0. Curves 1-3 are calculations for equilibrium flow with a stagnation temperature of 907°K (average for the density measurements), 835°K (thermocouple), and 730°K (delivery), respectively, and 4 is the calculation for nonequilibrium flow with $T_0 = 730°K$. As can be seen from this comparison, values of 907 and 835°K are high since they predict high k' in the stream, higher than given in the experiment. The closest values to the actual stagnation temperature are those obtained by the delivery method. Even more certain is the validity of selecting T_0 from delivery method data for maximum $p_0 d_*$ (schedule 3).

Equilibrium is observed in this experiment close to the nozzle edge, and the calculation coincides satisfactorily with the experiment.

LITERATURE CITED

1. H. Rabitz and S.-H. Lam, "Rotational energy relaxation in molecular hydrogen," J. Chem. Phys., 63, No. 8 (1975).
2. K. Koura, "Rotational distributions of N_2 in free jet and shock wave," in: Rarified Gas Dynamics, 11th Int. Symp. Proc., Paris; Commissariate à l'Energie Atomique, Vol. 2 (1979).
3. A. N. Vargin, N. A. Ganina, et al., "Rotational relaxation of molecular nitrogen in a freely expanding jet," Zh. Prikl. Mekhan. Tekh. Fiz., No. 3 (1979).
4. P. A. Skovorodko and R. G. Sharafutdinov, "Population kinetics for rotational levels in a nitrogen jet," Zh. Prikl. Mekhan. Tekh. Fiz., No. 5 (1981).
5. H. Ackenas and F. S. Sherman, "Structure and utilization of supersonic free jets in low-density wind tunnels," in: Rarified Gas Dynamics, 4th Int. Symp. Proc., Vol. 2, Academic Press, New York-London (1966).
6. A. I. Osipov, "Dynamics of a nonequilibrium gas," Teplofiz. Vysokykh Temp., 9, No. 6 (1971).
7. P. A. Skovorodko, "Rotational relaxation during expansion of a gas into a vacuum," in: Dynamics of Rarified Gases [in Russian], ITF SO Akad. Nauk SSSR, Novosibirsk (1976).
8. C. Nyeland and G. D. Billing, "Approximative treatments of rotational relaxation," Chem. Phys., 40, No. 1 (1979).

9. S. Lee and Y. S. Kim, "Study of the Ar–N_2 interaction. 2. Modification of the electron-gas model potential at intermediate and large distances," J. Chem. Phys., 70, No. 11 (1979).
10. G. V. Dubrovskii, V. A. Pavlov, and R. É. Mukhametzyanov, "Rotational excitation of diatomic molecules during collision with atoms," Inzh.-Fiz. Zh., 22, No. 2 (1984).
11. G. V. Dubrovskii and L. F. V'yunenko, "Theory of vibrational–rotational excitation of diatomic molecules within the framework of a generalized eikonal method," Zh. Eksp. Teor. Fiz., 80, No. 2 (1981).
12. R. E. Mukhametzyanov and V. A. Pavlov, "Analytical approximations of cross sections and rate constants for the case of R–T-relaxation in gases," Vestn. LGU. Matem., Mekhan., Astron., No. 19 (1983).
13. M. D. Pattengil and R. B. Berstein, "Surprisal analysis of classical trajectory calculations of rotationally inelastic cross sections for the Ar–N_2 system, influence of the potential energy surface," J. Chem. Phys., 65, No. 10 (1976).
14. M. H. Alexander, "Close-coupling studies of the orientation dependence of rotationally inelastic collisions," J. Chem. Phys., 67, No. 6 (1977).
15. R. T. Pack, "Close coupling test of classical and semiclassical cross sections for rotationally inelastic Ar–N_2 collisions," J. Chem. Phys., 62, No. 8 (1975).
16. V. A. Pavlov, G. V. Dubrovskii, and R. É. Mukhametzyanov, "Calculations of cross sections and rate constants of rotational excitation for the system Ar–N_2," Teplofiz. Vysok. Temper., 21, No. 5 (1983).
17. R. J. Cross, "Exponential time-dependent perturbation theory in rotational inelastic scattering," J. Chem. Phys., 79, No. 3 (1983).
18. A. E. De Pristo and H.Rabitz, "Scaling theoretic deconvolution of bulk relaxation data: state-to-state rates from pressure broadened line widths," J. Chem. Phys., 68, No. 4 (1978).
19. B. N. Borzenko, N. V. Karelov, et al., "Experimental study of the populations of rotational levels for molecules in a free nitrogen jet," Zh. Prikl. Mekhan. Tekh. Fiz., No. 5 (1976).
20. A. E. Belikov, A. E. Zarvin, et al., "Electron-beam diagnostics for nitrogen: multiquantum rotational transitions during excitation," Zh. Prikl. Mekhan. Tekh. Fiz., No. 3 (1984).
21. J. B. Anderson, "Molecular beams with nozzle sources," in: Molecular Beams and Low Density Gas Dynamics, Marcel-Dekker, New York (1974).
22. E. P. Muntz, "Static temperature measurements in a flowing gas," Phys. Fluids, 5, No. 1 (1962).
23. A. E. Zarvin and R. G. Sharafutdinov, "Rotational relaxation in a transition regime for free nitrogen jets," Zh. Prikl. Mekhan. Tekh. Fiz., No. 6 (1981).
24. D. A. Mel'nikov, Yu. G. Pirumov, and A. A. Sergienko, "Nozzles for reactive engines," in: Aeromechanics and Gas Dynamics [in Russian], Nauka, Moscow (1976).
25. G. Luijks, S. Stolte, and J. Reuss, "Molecular beam diagnostics by Raman scattering," Chem. Phys., 62 (1981).
26. A. E. Belikov, A. E. Zarvin, et al., "Disruption of a Boltzmann distribution for populations of rotational levels in free nitrogen jets," Zh. Prikl. Mekhan. Tekh. Fiz., No. 1 (1984).